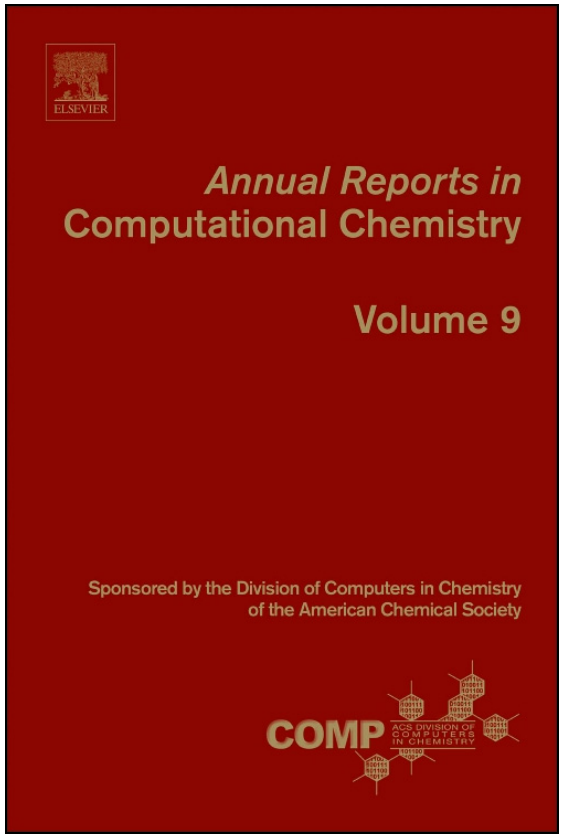

From: Chia-en A. Chang, Yu-ming M. Huang, Atomistic Modelling of Phosphopeptide Recognition for Modular Domains. In Ralph A. Wheeler, editors: *Annual Reports in Computational Chemistry,* Vol. 9,
Amsterdam: The Netherlands, 2013, pp. 61-84.
ISBN: 978-0-444-62672-1

CHAPTER THREE

Atomistic Modelling of Phosphopeptide Recognition for Modular Domains

Chia-en A. Chang[1], **Yu-ming M. Huang**
Department of Chemistry, University of California, Riverside, California, USA
[1]Corresponding author: e-mail address: chiaenc@ucr.edu

Contents

Abstract

This review aims at discussing the molecular details of binding specificity, promiscuity and mechanisms of phosphopeptide recognition to modular domains using computational tools. Protein–phosphoprotein interactions are the driving forces that underline multiple signalling events which are important in cellular function. Understanding protein–phosphopeptide recognition assists designing phosphopeptide sequences as inhibitors to manipulate protein–protein interactions for cell biology studies and therapeutics. Notably, the modular domain–phosphopeptide binding is mostly promiscuous and weak binding, which significantly differs from most protein–ligand binding systems used for drug design. In this chapter, we review recent advances in computational work for modular domain–phosphopeptide binding and knowledge gained for their binding mechanisms. We discuss the phosphopeptide binding of modular domains in DNA damage responses, FHA and BRCT, the smallest modular domain WW and the tyrosine kinase binding domain, such as Cbl–TKB that recognizes

Annual Reports in Computational Chemistry, Volume 9
ISSN 1574-1400
http://dx.doi.org/10.1016/B978-0-444-62672-1.00003-0

phosphotyrosine. We also discuss challenges and possible future directions for improving peptide design as inhibitors for phosphoprotein–protein binding.

1. INTRODUCTION

Protein function must be regulated and protein phosphorylation is one of the major tools that have developed to fill this need. Protein phosphorylation is widely exploited in DNA damage repair, signal transduction, cell growth and cell cycle regulation; the cascades of downstream signals can be triggered by grabbing a certain phosphoprotein *(1–6)*. Diverse arrays of modular domains recognize phosphoproteins by non-covalent binding that result in switch-like changes in protein function. The interactions between modular domains and their phosphoprotein partners are usually weak and transient, which tend to be underrepresented in high-throughput and computational studies. The domains are usually promiscuous proteins and can recognize more than one peptide sequence. Understanding these protein–peptide interactions is of great interest in a wide variety of applications such as molecular detection, inhibitor discovery and searching for binding partners. Promiscuous recognition at the molecular level usually involves different levels of conformational changes and numerous bond rotations *(7,8)*. However, the underlying mechanism that drives diverse ligands to dock into the same binding site of a protein is not fully understood.

The phosphoproteins are usually classified into two families: phosphotyrosine (pTyr)-containing and phosphoserine (pSer)/phosphothreonine (pThr)-containing sequences, which are phosphorylated and dephosphorylated by different categories of kinases (e.g. pTyr kinase and pThr/pSer kinase) and phosphatases *(9)*. Recent studies discovered a few modular domains that particularly recognize pThr/pSer- or pThr-containing sequences, such as the breast cancer-associated protein BRCA1 C-terminal (BRCT) repeats, WW domain, 14-3-3, WD40, polo-box and forkhead-associated (FHA) domain *(10–12)*. Domains such as the Src homology-2 (SH2) domain and phosphotyrosine kinase binding (TKB) domain mediate protein–protein interactions by targeting motifs that contain pTyr *(8,13,14)*.

The recent development of innovative algorithms has advanced knowledge of molecular recognition in phosphopeptide–modular domain systems. For example, advances in molecular dynamics (MD) simulations, various post-analysis methods and bioinformatics algorithms offer powerful tools

to study binding mechanisms (Figure 3.1), assist computer-based inhibitor design and predict phosphopeptide binding sites *(15–22)*. In this chapter, we discuss the mechanisms of binding various phosphopeptides to modular domains. Specifically, we ask how nature achieves both specificity and promiscuity in these important signal transduction systems.

2. METHODS

2.1. Atomistic molecular dynamics simulations

The classical MD simulation-based method is the most widely used tool of computational techniques. It is perhaps the least glamorous method, but in many cases, it is the most powerful method. It provides atomistic details of motions of a molecular system and inter- and intra-molecular interactions during a given simulation time period. MD involves the integration of Newton's equation of motion for a set of atoms. The solvent can be modelled either explicitly, which is more accurate but more expensive, or implicitly through use of approximations based on continuum electrostatics, which is less accurate and inexpensive. Molecular mechanics (MM) force fields such as the OPLS, AMBER and CHARMM are typically used in these simulations with fixed-charged models *(23–26)*. Parameters for phosphoresidues, such as pThr, pSer and pTyr, are also available *(27)*. Conventional MD simulations can be used in an unbiased manner, but they can only realistically probe nanosecond-order timescales. Other biased sampling methods, such as targeted MD, accelerated MD and torsion angle-based sampling methods can be used to explore conformational changes more efficiently or to compute binding energies *(28–31)*. MM methods cannot be used to study catalysis, and combined quantum mechanics (QM) and MM have been used to study the phosphorylation reaction and how phosphorylation may affect catalysis. Because our focus is non-covalent binding and phosphopeptide recognition, we do not discuss QM/MM methods.

2.2. Bioinformatics tools

A modular domain may be identified in many different proteins, and although their sequences may not be highly identical, the domains share the same structure features. For example, the FHA domain has been identified in more than 2000 proteins from the Pfam database *(32,33)*, and the structure is conserved. Moreover, modular domains may form complexes with several different phosphopeptide sequences and the complex

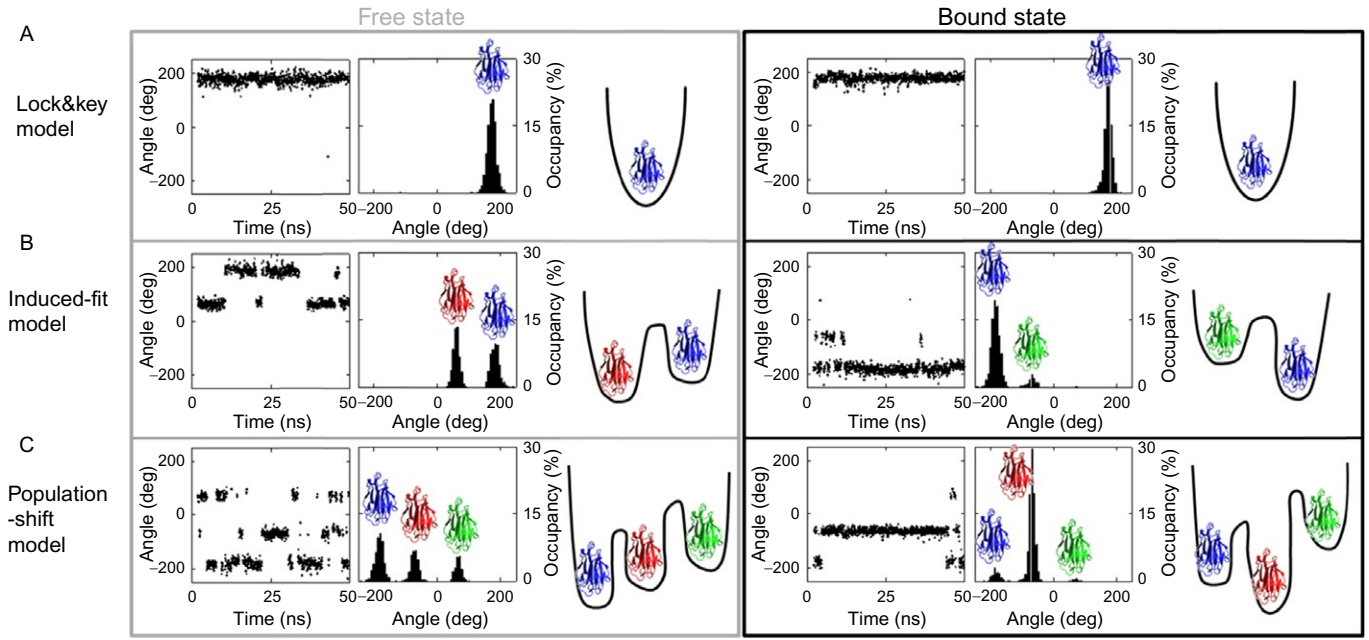

Figure 3.1 Three hypothesis models, lock and key (A), induced-fit (B) and population-shift/conformation-selection (C), to represent conformational changes in free and bound state. We plot the specific dihedral angle with simulation time and make it as a histogram distribution. The proteins coloured as blue, red and green indicate different conformations.

conformations may not be highly identical. X-ray crystallography and nuclear magnetic resonance (NMR) provide the highest resolution structural information for the domain–phosphopeptide complexes but are also the most difficult and time consuming to obtain. Bioinformatics methods provide fast and powerful tools to model the binding of various peptide sequences to a modular domain of a protein or different proteins. Homology modelling and multi-sequence alignment tools using well-developed Web sites are popular methods to build models for domains without experimental structures. The first step of homology modelling methods begins with the selection of suitable structural template(s) from the Protein Data Bank (PDB). Web servers such as SWISS-MODEL provide user friendly interface to search for templates *(34–36)*. The server also provides a template library, the SWISS-MODEL template Library (ExPDB), which is derived from the PDB. A wide variety of alignment tools and homology modelling packages and servers, such as T-coffee, MODELLER, Sybyl, Prime and ICM, are also commonly used to develop a homology model based on the selected template(s) *(37)*.

2.3. Coarse-grained Brownian dynamics simulations

The introduction of a phosphate group generally carries a −2 charge at physiologically pH. The large electrostatic perturbation can affect association processes of the phosphopeptide or phosphoprotein by increasing the electrostatic steering forces and/or alter protein structure and interactions. To study molecular association processes and large-scale conformational changes are being accomplished through the use of course-grained (CG) model and several CG models have been implemented in current MD or Brownian dynamics (BD) software *(38–41)*. Many CG models have been proposed over the years, for example, see refs. *(42–56)*. In this chapter, we discuss the use of BD algorithm with a one-bead CG model developed by Tozzini and McCammon as an example to investigate phosphopeptide–domain association *(57,58)*.

3. EXAMPLES OF MODELLING OF PHOSPHOPEPTIDE AND MODULAR DOMAIN BINDING

3.1. FHA domains: a domain that specifically recognizes phosphothreonine

A unique feature of FHA domains is that they can differentiate pThr-containing peptides from pSer-containing peptides, although the difference

is only one methyl group *(59–63)*. Most pSer/pThr-binding modules, such as BRCT and WW domains, can specifically bind to short pSer/pThr-containing motifs equally well. Not unsurprisingly, one more methyl group of Thr has few effects on the overall binding and molecular recognition. Not only in peptide–protein binding, a recent literature analyses more than 2000 cases of methyl effects on protein-drug like compound and the results shows that less than 10% cases, containing a methyl group, results in 10-fold or greater binding affinity boost *(64)*. However, most FHA domains recognize only pThr residue in target proteins, and the substitution of pSer for pThr in model peptides severely weakens binding. Because Ser/Thr kinase phosphorylates both residues, the FHA domain can efficiently reduce potential interaction sites by specifically binding to pThr-containing regions and this recognition may function as a filter to further select the protein partner.

3.1.1 Topological and 3D Structures of FHA

The FHA domain is associated with proteins of diverse functions in different organisms. For example, the FHA1 domain in Rad53 protein, the Rad53–FHA1 domain, interacts with phosphorylated Rad9 in response to DNA damage, and the Dun1–FHA domain interacts with SCD1 of Rad53, which leads to activation of Dun1 in response to DNA damage response *(65,66)*. Phosphopeptide sequences discussed in this chapter are listed in Table 3.1. Although the sequence identity between the FHA from different proteins is low, for example, the sequence identities of Dun1–FHA and the Ki67–FHA to Rad53–FHA1 are both 34%, the structure of the FHA domain is well conserved: a twisted β sandwich of 11 well-defined β sheets, 5 in the front and 6 at the back (Figure 3.2) *(61,62,67,75–79)*. Generally, the domain contains ~120–140 residues, but only 5–10 residues are conserved. Six loops connected to the secondary β strands constructing the pThr-binding site are the main difference between distinct FHA domains. Experimental structures show that the synthetic peptides bind to the loops between β3–β4, β4–β5, β6–β7 and β10-β11 and the conserved pThr-binding site locates between loops β4–β5 and β6–β7 (Figure 3.2) *(61,62)*.

3.1.2 Revealing the Specificity of the pThr-Binding Site in FHA Domain

A unique feature of the FHA domain family is the use of loops to recognize peptide sequences. Loops are typically considered flexible regions in proteins, but analysis of FHA domain conformations suggests a conserved

Table 3.1 List of phosphopeptide sequences

No.	PDB ID	Domain	Method	K_d (μM)	Sequence	References
1	1G6G	Rad53-FHA1	X-ray	0.53	LEV(pT)EADATFAK	*(61)*
2	1K3Q	Rad53-FHA1	NMR	0.30	SLEV(pT)EADATFVQ	*(65)*
3	2JQL	Dun1-FHA	NMR	0.30–1.2	NI(pT)QP(pT)QQST	*(66)*
4	2AFF	Ki67-FHA	NMR	0.077	KTVD(pS)QGP(pT)PVC(pT) **PTFLERRKSQVAE**LNDDDKDD**EIVFK**QPISC	*(67)*
5	1F8A	Pin1-WW	X-ray	34	Y(pS)PT(pS)PS	*(68)*
6	1T2V	BRCA1–BRCT	X-ray	0.40	AAYDI(pS)QVFPFA	*(69)*
7	1T29	BRCA1–BRCT	X-ray	0.90	ISRST(pS)PTFNKQ	*(70)*
8	1Y98	BRCA1–BRCT	X-ray	3.7	PTRVS(pS)PVFGA	*(71)*
9	3COJ	BRCA1–BRCT	X-ray	5.2	PQ(pS)PTFPEAG	*(72)*
10	2CBL	Cbl–TKB	X-ray	12.2	TLNSDGpYTPEPA	*(73)*
11		Cbl–TKB	X-ray[a]	3.7	pYTPEP	*(74)*
12		Cbl–TKB		>37[b]	pYTP(ptE)P	

Secondary structure, α-helix and β-sheet are labelled as bold.
[a]Manually truncated the long peptide from 2CBL.
[b]Unpublished data.

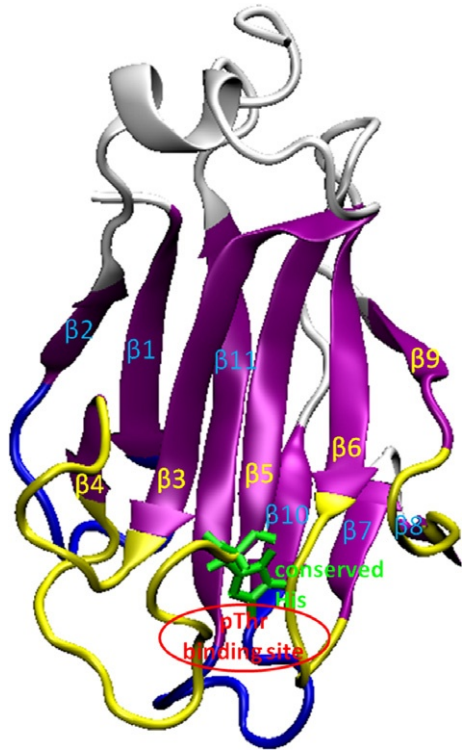

Figure 3.2 FHA structure from a MD snapshot. Loops/β-sheets in the front and at the back are labelled as yellow and blue, respectively. Other loops which do not have direct contacts with peptide are shown in white. Green and red represent conserved His- and pThr-binding cavity.

structure in the main pThr-binding site formed by two loops between β3–β4 and β6–β7 (see Figure 3.2). Recent studies substituted pThr with pSer *in silico* and performed interaction energy calculations and analysis of configuration space to illustrate why the methyl group plays the crucial role in determining binding *(80)*.

Although experimental structures demonstrate a pocket to accept the pThr methyl group, the static conformation cannot ascertain that pSer fails to form equally good interactions with the nearby residues because the protein is dynamic and may fill the space of a methyl group by slightly changing the protein conformations. MD simulations show that the cavity is highly suited to pThr, and the local flexibility is changed because of the lack of

the methyl group in pSer-containing phosphopeptides. Most side-chain dihedrals stay in the same rotamer states for both pSer/pThr residues, but the second pThr side-chain dihedral angle (see Figure 3.3A) differs. Figure 3.3 shows the distribution of the side-chain dihedral angle of pThr and pSer in Rad53–FHA1 peptide. The dihedral of pSer deviates from pThr with a significant angle shift and also has wider distribution, so the dihedral is more flexible. Clearly, the methyl group of pThr allows the phosphoresidue to fill the entire pocket of the binding site, and no room is available for spacious vibration of the pThr side chain. In contrast, the space released by the absence of methyl group cannot be adequately filled by protein side chains, which creates room for the dihedral of pSer to be more flexible. Although side chains of the dual loops are mobile, the conserved His, located at the N-terminus of β5, uses the imidazole ring and polar interactions to form stable interactions with residues of loops β4–β5 and β6–β7. Note that the His shown in Figure 3.2 is conserved in all FHA domains, although it does not directly interact with a phosphopeptide. Interestingly, MD simulations explain how FHA makes use of the conserved His to stabilize the dual loop and form a structural room to dock the methyl group and discriminate pThr/pSer.

Interaction energy calculations, so-called MM/PBSA calculations, quantify the attraction forces between pSer/pThr and residues around the phosphoresidue, which reveal how FHA can discriminate between them. Although the only difference between the Thr and Ser residue is one methyl group, which is usually considered not significant, atomistic modelling indicates that the methyl group directly interacts with residues of loops β4–β5 and β6–β7 of the FHA domain (see Figure 3.3). The local interaction energy is less favourable when pThr is replaced by pSer and shows that van der Waals interactions are weakened considerably by the lack of a single methyl group of pSer; the loss of the van der Waals attraction can be weakened by ~3 kcal/mol. The interaction between the methyl group of pThr and the nearby residues is unlikely to be 3 kcal/mol, but instead, the computed energy reveals the crucial role of the methyl group to stabilize the complex conformation locally. Interestingly, although the phosphate group of pSer still retains hydrogen bonding between the nearby residues of FHA, the electrostatic attractions are still weakened. This again supports that solely forming H-bonds between the phosphate group of the phosphoresidue is not enough for phosphopeptide and FHA domain binding, and lacking the methyl group destabilizes the complex. Fewer contacts can be formed when pSer is present in the peptide.

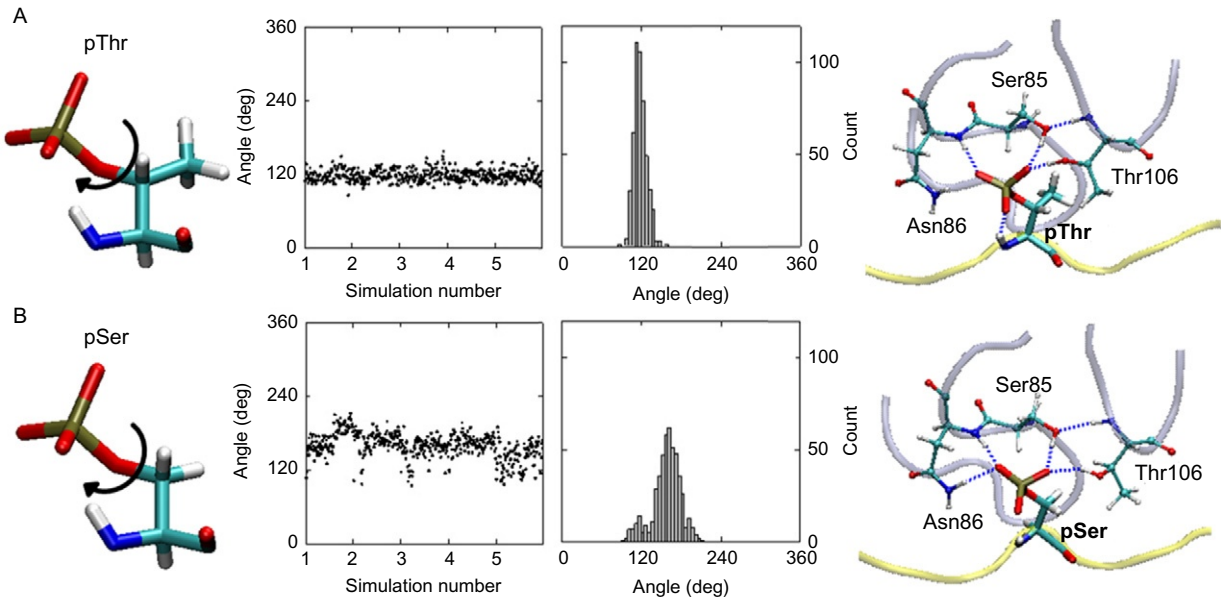

Figure 3.3 The second side-chain dihedral angle of pThr (A) and pSer (B). We plot the angle distribution from five individual MD simulations; each simulation is 1 ns. The MD snapshots show the detailed interactions between phosphoresidue and FHA domain. Blue dash lines indicate charge–charge attractions.

3.2. WW: The smallest modular domain recognizes both pThr and pSer

WW domains are the smallest, naturally occurring modular domains that have only about 40 residues *(4)*. Due to the small size and compact fold, WW became an attractive model for studying protein stability, protein design and prediction of binding phosphopeptides for a specific WW domain sequence *(68,81)*. They are found in many different proteins; for example, the WW domain in Pin1, Pin1-WW, is essential for mitotic progression *(82)*.

3.2.1 Topological and 3D structures of WW

The name refers to two tryptophan (W) residues that are 20–22 residues apart and are present in most WW domains in sequence analysis. Not all WW domains function as phosphopeptide binding modules, but a subgroup of the domain recognizes proline (Pro)-containing phosphopeptides and folds into three anti-parallel β stands. As shown in Figure 3.4, Arg21 and Ser22 residues in the loops between β1 and β2 are the phosphate group recognition sites *(4,5,83)*. It specifically binds to pThr-Pro- or pSer-Pro-containing motifs with slightly higher affinity for pThr-Pro-containing peptides *(81)*. For example, in the Pin1-WW domain, the aromatic rings of Tyr23 and Trp34 define a steric clamp to confer a Pro adjacent to pSer/pThr *(83)*.

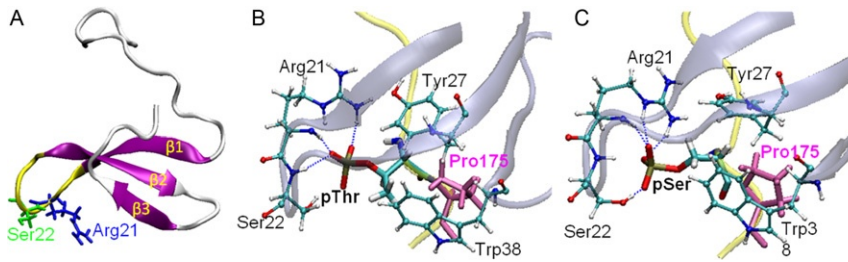

Figure 3.4 (A) WW domain structure. Yellow indicates peptide binding loop. Two key residues which directly bind to phosphoresidue are represented in blue and green. The MD snapshot that shows pThr and pSer-containing peptide binding is shown as (B) and (C), respectively.

3.2.2 Intrinsic dynamics of apo WW domain and pThr and pSer recognition

Flexibility helps accommodate the promiscuous binding properties of modular domains (*1,12*). For domains that show obvious two-state—the free and bound—conformations, such as Pin1-WW, the free domains may pre-exist holo-like conformations. NMR relaxation experiments have emerged as a premier tool for revealing the location and timescale of conformation ensembles for free domains and the transitions between the free and bound states (*84–86*). However, detailed atomistic observations still need to rely on computational simulations. MD simulations and Markov state models (MSMs) show that the apo Pin1-WW domain has intrinsic dynamics, resulting in conformational equilibria between holo-like and pre-exist alternative conformers for phosphopeptide recognition. The analysis of correlated motions also suggests that the domain may help couple the substrate binding site on the WW domain to the one on the catalytic domain (*87*).

Although it is common that proteins treat Ser and Thr as a similar residue, knowing how WW has non-specific pThr/pSer recognition with a specific Pro residue is of interest. The WW domain utilizes the combination of a single loop with β-sheet, which allows effectively side-chain rearrangement to accept both pSer and pThr. Although the WW domains are able to recognize both pSer- and pThr-containing peptides, binding energy calculations from MD simulations suggest that the domain favours pThr because of the more preferable van der Waals attractions. This trend is in agreement with experimental results (*81,82*). As shown in Figure 3.4B and C, two conserved aromatic residues of the domain, Tyr and Trp, create a cavity, but no side chains of phosphopeptides could nicely fit into the cavity during MD simulations. Interestingly, the conserved Pro residue adjacent to the phosphoresidue is clamped by Tyr and Trp, which stays in the cavity and further restricts nearby phosphopeptide conformations. The confined region formed by rings of Tyr, Trp and Pro is conserved regardless of the presence of pSer or pThr (see Figure 3.4B and C), which explains the crucial roles of Pro. Because of the bulky ring conformations, an empty space is observed during the course of the MD simulations. The empty space can be partially filled by the methyl group of pThr, thus resulting in more favourable van der Waals interactions and a less flexible side chain while pThr is binding. However, the Pro residue but not the methyl group of pThr primarily occupies the cavity in phosphopeptide recognition. Therefore, the domains do not show significant discrimination between pSer and pThr. The hydrogen bonds between pThr or pSer and the nearby residues are always present

during the simulations, suggesting the important role of phosphate for overall binding affinities.

3.3. BRCT: Case study for binding mechanisms

Promiscuous proteins are commonly observed in biological systems, and this characteristic makes it possible to use limited numbers of domains to regulate considerably more binding partners through protein phosphorylation. In addition to the ability to recognize phosphopeptides with similar polar or non-polar features, the binding interface of some domains can accommodate diverse peptide sequences, including both polar *and* non-polar phosphopeptides, by applying different binding mechanisms. For this chapter, we use the BRCT domain of BRCA1, BRCA1–BRCT, as a model system to study binding mechanism for promiscuous recognition (see Table 3.1 for phosphopeptide sequences).

Because of the promiscuous nature, a domain may utilize different binding mechanisms when it recruits different phosphopeptide sequences. Typically, the binding mechanisms may be divided into three representative postulates: lock and key, induced-fit and population-shift/conformational-selection model *(88,89)*. The basic mechanism of lock and key model has been introduced for a long time *(90)*. In this postulate, only correctly pre-organized ligands are capable to fit into the active site of the lock, which indicates that the conformations would not change during binding (Figure 3.1A) *(91–93)*. Since not all cases can be adequately explained by the rigid lock model, another assumption, induced-fit theory, has been proposed and showed that biomolecules are rather flexible structures in which the conformation can be reshaped and distorted to optimize interactions with partners (Figure 3.1B) *(88,89,91)*. Experiments also support another mechanism, termed population-shift or conformational-selection model. In this model, free protein or ligand has a large number of conformations pre-existing in the native state. After binding, the structure is perturbed and thus the properties of population switch (Figure 3.1C) *(88,94)*. Because the BRCA1–BRCT domain recognizes sequences with mainly polar, non-polar and mixed residues, it serves as a good model system to study binding mechanisms to gain knowledge in peptide design.

3.3.1 Topological and 3D structures of BRCT

The BRCT domains are protein-binding modules originally discovered as a domain conserved in multiple DNA damage-response proteins *(95,96)*. This vital modular domain system, BRCA1–BRCT, shows strong binding

affinity with different types of pSer peptides *(69,70,97)*. The BRCT domains are often found in the form of tandem repeats (see Figure 3.5A). A single domain in the BRCT fold is packed with four parallel β sheets with a pair of α helices (α1 and α3) flanked on each side and one helix on the opposite face (Figure 3.5A) *(98)*. The overall structure of the tandem repeats BRCT domain from different protein families is conserved: a cluster of hydrophobic residues locates at the interface between the two repeats *(97)*. The mutation of the BRCT will cause cancers. Unlike the domain parts, the linker connecting two repeats is more diverse, with poorly defined crystal structures, which suggests flexibility of the linker region *(99)*. The BRCA1 protein is a tumour suppressor and is involved in multiple cellular functions such as DNA repair and signal transduction. Besides BRCA1, many other proteins are known to contain single or multiple BRCT domains, with 90–100 amino acid residues in each domain. In this chapter, we focus on BRCA1–BRCT. Similar to WW, not all BRCT domains function as phosphopeptide-binding modules. However, the BRCA1–BRCT domains recognize pSer-X-X-Phe motifs (X means several different amino acids) that have been demonstrated to bind the phosphorylated DNA helicase BACH1, phosphorylated Abraxas and the phosphorylated transcriptional corepressor CtIP *(11,70–72)*.

3.3.2 Mechanistic insights into BRCT–phosphopeptide recognition

MD simulations can efficiently sample dihedral rotations in both free and bound domain, which provides us the useful information about which mechanism that the interface will apply to recognize a given phosphopeptide sequence. The rotamer states of each residue in the binding site of BRCT and four different phosphopeptides can be counted from the MD simulations. Modelling results show that the backbone dihedral angle mostly stayed in a single energy well and remained the same with or without phosphopeptide binding, and as expected, the side-chain dihedrals were more flexible and usually had more than one rotamer state. Although, commonly, ligand binding decreases the number of available rotamer states, the rotamer states of BRCT and the phosphopeptides can be increased or remain unchanged in their free and bound states (Figure 3.5B). Upon binding to BRCA1–BRCT, phosphopeptide 6 showed new rotamer states of a number of residues shown in Figure 3.5C, which suggests that the peptide can efficiently rearrange itself to fit into the binding interface of BRCT. New rotamer states of several non-polar residues of phosphopeptide 6 are induced by binding a hydrophobic binding groove. This new dihedral angle

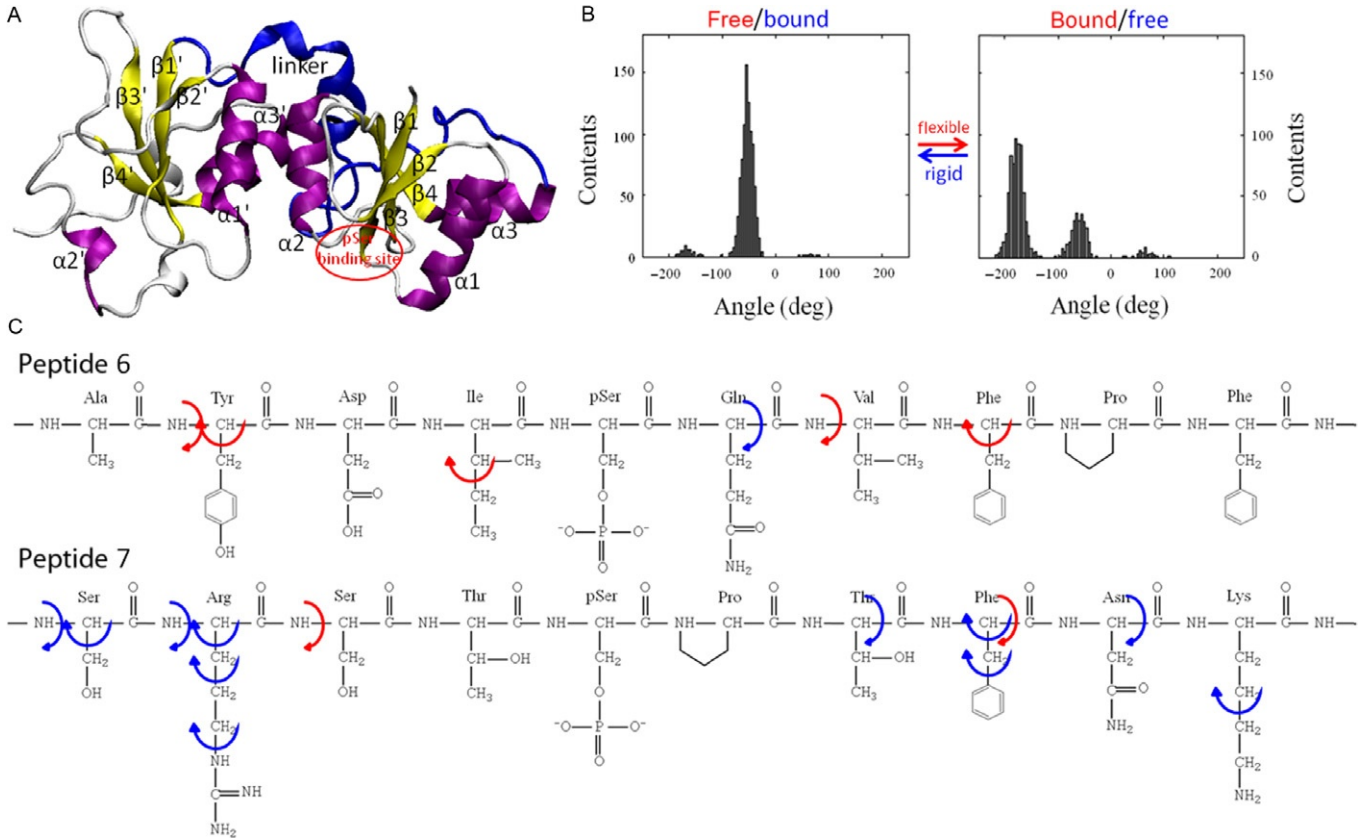

Figure 3.5 (A) BRCT structure. (B) Dihedral angle distribution to represent conformations can be either more flexible or rigid in bound state. (C) Two peptide sequences with all rotatable bonds. Red and blue show that, after binding, dihedrals become more flexible and rigid, respectively.

distribution is a case that fits in the induced-fit model (Figure 3.1B). For phosphopeptides 7, 8 and 9, despite new rotamer states and different conformations being found in the bound complexes, most dihedral angles are less mobile and have fewer rotamer states, which utilizes the "conformational selection" or "population-shift" mechanism (Figures 3.1C and 3.5C). Therefore, highly charged (phosphopeptide 7) and mixed (phosphopeptides 8 and 9) side chains are more flexible in a water environment, but the movement is restrained when the phosphopeptides bind to the hydrophobic groove of BRCT. Despite the decreased flexibility of BRCA1–BRCT and the phosphopeptides, both parties can adopt different conformations for peptide binding through moderate side-chain arrangement. Moreover, population of some side chains of phosphopeptides and BRCA1–BRCT does not change during binding and the side chains preorganize as a lock and a key illustrated in Figure 3.1A.

Different from the Pin1-WW domain, the MD results show preorganization of the backbone of BRCA1–BRCT and moderate arrangements of side chain to create the optimal binding environment. Three binding models for explaining molecular recognition are all observed in MD simulations. One can observe that a part of dihedral angle population does not have significant changes during ligand binding, which is related to the lock and key model. In more hydrophobic environments, in which binding enables non-polar side chains to have more degrees of freedom to rotate, the recognition of BRCT domain and phosphopeptide tends to proceed by the induced-fit model. However, the population-shift model is commonly found in polar interactions due to charge–charge interactions that have preferred direction. Moreover, the binding region of both protein and phosphopeptide is able to show more rigid and flexible while interacting with polar and non-polar partners, respectively. The example provides insight into recognition in phosphopeptides with different features.

3.3.3 *Modelling the phosphorylation effect on diffusional association using coarse-grained BD simulations*

Long-range electrostatic steering often plays a key role in ligand–protein association, governing the association rate constants *(100–102)*. Therefore, it is of interest to know whether the charged phosphate group accelerates the diffusional association process of the peptide. Because of the long timescales involved in modelling the diffusion processes, simulations using classical atomistic models may be impractical, and coarse-grained models are useful

tools to study molecular associations. BD simulations using a CG model were therefore used to study the effect of phosphorylation on the binding kinetics for peptides 6 and 7 from the phosphate group with and without the negative charge. Adding the phosphate group increased the net charge of the peptide by −2. Since the BRCT domain carries a −5 unit of formal charge, simulating the average association time showed no advantage in electrostatic steering attractions. Unexpectedly, although BRCT fails to form a complex with non-phosphopeptides, addition of the phosphate group demonstrates that peptides took two to three times longer to find the binding pocket and orient themselves to the final bound state. The positively charged residues in the linker region of BRCT temporarily kept the phosphopeptides locally, and sometimes the peptides stayed in a positive-charged patch longer than 15 μs. As a result, the total traffic time along the BRCT surface was increased, thus resulting in a longer BRCT–peptide association process.

It is worth noting that proteins containing the BRCT domain are significantly larger than the domain alone, which may have different charge distributions on the protein surface as well. Therefore, the example showing a slowdown in the overall BRCT–peptide association by adding the phosphate group could be an artefact of considering only the BRCT domain. Nevertheless, the results suggest that solely increasing the net charge of a molecular system may not always benefit the overall association processes, and the charge patches on a protein surface may temporarily trap the ligand. Although the phosphate group is not able to speed up phosphopeptide association, the charge interactions can efficiently guide the phosphopeptide to the correct orientation. The phosphate group stabilizes the bound BRCT–phosphopeptide complex, which is shown in both atomistic MD and CG BD simulations.

3.4. Cbl–TKB: long or short phosphopeptides?

Systematic development of short peptide or chemical inhibitors that perturb protein–protein interactions, now becoming more feasible for both cell biology and therapeutics, will benefit from modelling of peptide–protein recognition. These compounds can serve as valuable tools to dissect the complex signalling network in cellular processes and have advantages over classical biochemical techniques, such as mutagenesis, silencing RNA and gene knockouts. Typically, longer peptides provide more contacts for attraction than shorter ones. However, unusually, some truncated shorter peptides

show similar or even-increasing binding affinities to their protein partner than their long peptide parent. These short peptides serve as an ideal starting point for developing inhibitors of protein–protein interactions. Because of their sizes and feasible flexibility, computational studies can be used for fundamental studies of peptide–protein recognition and as powerful tools for *in silico* peptide design.

3.4.1 Topological and 3D structures of Cbl–TKB

The casitas B-lineage lymphoma (Cbl) family proteins are evolutionarily conserved attenuators of protein tyrosine kinase signalling, whose aberrant activation is frequently associated with oncogenesis. Loss of normal Cbl functions is believed to lead to unregulated activation of regulation and cellular transformation *(103)*. Cbl proteins interact with tyrosine kinases and the binding is a phosphorylation-driven event. The N-terminal tyrosine kinase binding domain (TKB) of Cbl, Cbl–TKB, directly interacts with cognate phophotyrosyl peptide motifs of protein tyrosine kinases to regulate protein tyrosine kinase signalling *(14)*. The TKB structurally resembles an SH2-like subdomain but requires a four-helix bundle (4H) and an EF-hand subdomain to accomplish binding (Figure 3.6) *(73)*. Regulation of tyrosine kinase signalling is now widely recognized—based on inhibiting tyrosine kinase and Cbl–TKB binding with peptide inhibitors—as an oncogenesis-driving mechanism amenable to targeted therapies.

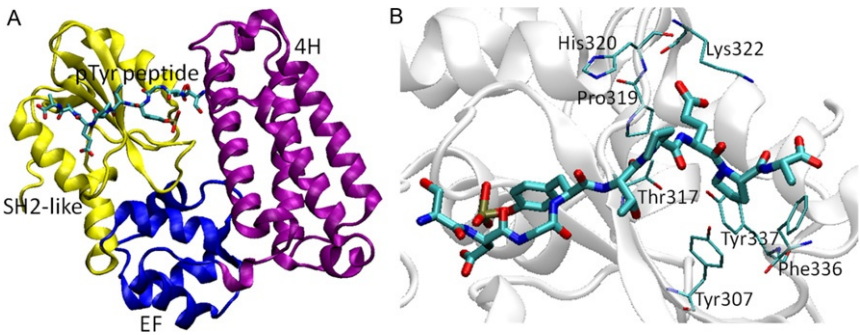

Figure 3.6 (A) TKB structure taken from PDB ID: 2CBL. (B) Zoom-in structure of interactions between phosphopeptide and Cbl–TKB domain. Phosphopeptide tail can interact with several residues from SH2-like domain.

3.4.2 A twist and unusual increase in affinity from phosphopeptide truncation

Previous experiments characterized the Cbl–TKB binding site for the protein tyrosine kinase, and the domain recognizes various 12-mer phosphopeptides. The shortest one, a 10-mer phosphopeptide, has been identified from the CSF-1R protein *(74,104)*. Hydrogen binding between the phosphate group of the conserved tyrosine and nearby protein side chains plays a crucial role in binding. In addition, both termini, especially the C-terminus, form interactions with the domain. Experiments showed that Cbl–TKB can bind threefold tighter to a pentapeptide pYTPEP ($K_{eq} = 3.7$ μM) than to its parent phosphopeptide ($K_{eq} = 12.2$ μM), TLNSDGpYTPEPA identified in protein tyrosine kinase ZAP-70, where pY is phosphotyrosine *(105)*. Observing the bound state of the lead peptide inhibitor suggested that the pentapeptide adopts a poly-L-protein type II (PPII) helix; thus the successful binding may be related to the consequences of conformational constraint. Therefore, hypothesizing that a peptide with a pre-organized PPII conformation should be favourable, a new pYTP(ptE)P peptide was synthesized and tested there. In this designed peptide, glutamic acid (E) is replaced by an unnatural amino acid termed ptE and it is estimated that this pre-organization of both the backbone and side chain to the bound conformation in the pYTP(ptE)P peptide could result in nearly an order of magnitude increase in activity. NMR studies for the ptE containing peptide showed that the P(ptE)P region adopted the PPII conformation. However, biochemical assays showed that the new pYTP(ptE)P peptide lost over an order of magnitude of binding affinity with Cbl–TKB.

MD simulations were used to investigate why the designed pre-organized and rigid short peptide unexpectedly failed to bind more strongly than the lead peptide. Studies of the dynamics and energy calculations show that peptide binding to Cbl–TKB involves induced fit. To achieve the final bound conformation induced by peptide binding, the protein and peptide undertake multiple dihedral rotations. In addition, the final bound state is not limited to only one conformation similar to existing crystal structures. The modelling work shows that ptE residues are exposed to solvent and may orient away from productive TKB–Cbl interaction, which is the likely cause for the observed loss of activity (Figure 3.7). As a result, over-rigidifying both backbone and side-chain motions in the pYTP(ptE)P peptide reduces the local flexibility in the bound complex and introduces more unfavourable conformational changes in order to adopt the rigid peptide. Experiments in this phosphopeptide-domain system argue that the rules

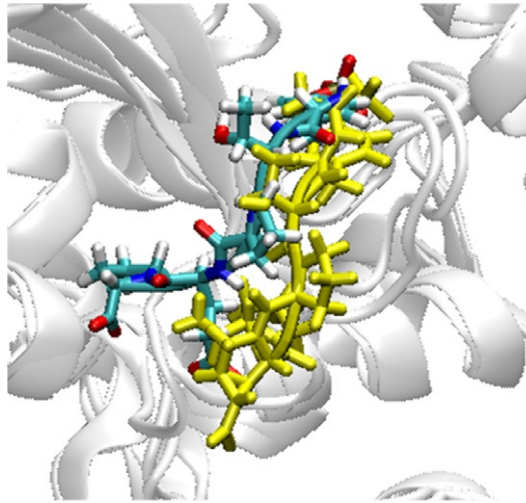

Figure 3.7 An MD snapshot of Cbl–TKB and peptide 11 (coloured) and 12 (yellow).

governing the design of potent inhibitors for interrupting protein–protein interactions are not yet fully defined. Due to the small number of examples reported in the literature, we highlight the lack of generality of these rules that scientists may rely upon to design good peptide inhibitors.

4. CONCLUDING REMARKS

Understanding phosphopeptide–modular domain recognition is a key to design peptides or peptidomimetic compounds to manipulate protein function involved in various signal transduction cascades. This review focuses on promiscuous and weak-binding protein modular domains that mediate signal transduction. These systems are different from most protein–ligand binding systems used for drug design; most drugs need to bind specifically and tightly to their target proteins. Moreover, weak binding may allow a system to be more flexible and respond faster, which has biological significance such as in DNA checkpoint signalling. From the literature, modelling tools such as MD simulations are widely applied to study the phosphopeptide–domain recognition. The atomistic detailed modelling work computed binding energies, investigated conformational changes of the molecules and modelled phosphopeptide association processes. However, because of the complex nature and highly flexible systems, the rules

determining successful design of phosphopeptides are not fully identified yet. Further studies, including more thoroughly understanding of binding mechanisms, efficient conformational searches and accurate binding affinities prediction will assist structure-based phosphopeptide design.

ACKNOWLEDGEMENTS

We thank support from the National Science Foundation (MCB-0919586) and Steven Ahrendt for valuable comments on the manuscript.

REFERENCES

1. Seet, B. T.; Dikic, I.; Zhou, M.-M.; Pawson, T. *Nat. Rev. Mol. Cell Biol.* **2006**, *7*, 473–483.
2. Westheimer, F. H. *Science* **1987**, *235*, 1173–1178.
3. Yaffe, M. B.; Cantley, L. C. *Nature* **1999**, *402*, 30–31.
4. Yaffe, M. B.; Smerdon, S. J. *Structure* **2001**, *9*, R33–R38.
5. Yaffe, M. B.; Smerdon, S. J. *Annu. Rev. Biophys. Biomol. Struct.* **2004**, *33*, 225–244.
6. Jorgensen, C.; Linding, R. *Brief. Funct. Genomic. Proteomic.* **2008**, *7*, 17–26.
7. Chang, Chia-en. A.; McLaughlin, W. A.; Baron, R.; Wang, W.; McCammon, J. A. *Proc. Natl. Acad. Sci. U. S. A.* **2008**, *105*, 7456–7461.
8. Nachman, J.; Gish, G.; Virag, C.; Pawson, T.; Pomes, R.; Pai, E. *Plos One* **2010**, *5*, e11215.
9. Virshup, D. M.; Shenolikar, S. *Mol. Cell* **2009**, *33*, 537–545.
10. Diella, F.; Haslam, N.; Chica, C.; Budd, A.; Michael, S.; Brown, N. P.; Trave, G.; Gibson, T. J. *Front. Biosci.* **2008**, *13*, 6580–6603.
11. Mohammad, D. H.; Yaffe, M. B. *DNA Repair (Amst.)* **2009**, *8*, 1009–1017.
12. Pawson, T.; Nash, P. *Science* **2003**, *300*, 445–452.
13. McLaughlin, W. A.; Hou, T. J.; Wang, W. *J. Mol. Biol.* **2006**, *357*, 1322–1334.
14. Lupher, M. L.; Reedquist, K. A.; Miyake, S.; Langdon, W. Y.; Band, H. *J. Biol. Chem.* **1996**, *271*, 24063–24068.
15. Karplus, M.; McCammon, J. A. *Nat. Struct. Biol.* **2002**, *9*, 646–652.
16. Hou, T. J.; Wang, J. M.; Li, Y. Y.; Wang, W. *J. Chem. Inf. Model.* **2011**, *51*, 69–82.
17. Gan, W. X.; Roux, B. *Proteins Struct. Funct. Bioinform.* **2009**, *74*, 996–1007.
18. Hou, T. J.; Zhang, W.; Case, D. A.; Wang, W. *J. Mol. Biol.* **2008**, *376*, 1201–1214.
19. McClendon, C. L.; Friedland, G.; Mobley, D. L.; Amirkhani, H.; Jacobson, M. P. *J. Chem. Theor. Comput.* **2009**, *5*, 2486–2502.
20. Ai, R.; Fatmi, M. Q.; Chang, C. E. A. *J. Comput. Aided Mol. Des.* **2010**, *24*, 819–827.
21. Narayanan, A.; Jacobson, M. P. *Curr. Opin. Struct. Biol.* **2009**, *19*, 156–163.
22. Joughin, B. A.; Tidor, B.; Yaffe, M. B. *Protein Sci.* **2005**, *14*, 131–139.
23. Jorgensen, W. L.; Maxwell, D. S.; TiradoRives, J. *J. Am. Chem. Soc.* **1996**, *118*, 11225–11236.
24. Okur, A.; Strockbine, B.; Hornak, V.; Simmerling, C. *J. Comput. Chem.* **2003**, *24*, 21–31.
25. Hornak, V.; Abel, R.; Okur, A.; Strockbine, B.; Roitberg, A.; Simmerling, C. *Proteins Struct. Funct. Bioinform.* **2006**, *65*, 712–725.
26. Vanommeslaeghe, K.; Hatcher, E.; Acharya, C.; Kundu, S.; Zhong, S.; Shim, J.; Darian, E.; Guvench, O.; Lopes, P.; Vorobyov, I.; MacKerell, A. D., Jr. *J. Comput. Chem.* **2010**, *31*, 671–690.
27. Homeyer, N.; Horn, A. H. C.; Lanig, H.; Sticht, H. *J. Mol. Model.* **2006**, *12*, 281–289.
28. Barducci, A.; Bonomi, M.; Parrinello, M. *Wiley Interdiscip. Rev. Comput. Mol. Sci.* **2011**, *1*, 826–843.

29. Larsson, P.; Hess, B.; Lindahl, E. *Wiley Interdiscip. Rev. Comput. Mol. Sci.* **2011**, *1*, 93–108.
30. Wang, Y.; Harrison, C. B.; Schulten, K.; McCammon, J. A. *Comput. Sci. Discov.* **2011**, *4*, 015002.
31. Hamelberg, D.; Mongan, J.; McCammon, J. A. *J. Chem. Phys.* **2004**, *120*, 11919–11929.
32. Punta, M.; Coggill, P. C.; Eberhardt, R. Y.; Mistry, J.; Tate, J.; Boursnell, C.; Pang, N.; Forslund, K.; Ceric, G.; Clements, J.; Heger, A.; Holm, L.; Sonnhammer, E. L. L.; Eddy, S. R.; Bateman, A.; Finn, R. D. *Nucleic Acids Res.* **2012**, *40*, D290–D301.
33. Sammut, S. J.; Finn, R. D.; Bateman, A. *Brief Bioinform.* **2008**, *9*, 210–219.
34. Arnold, K.; Bordoli, L.; Kopp, J.; Schwede, T. *Bioinformatics* **2006**, *22*, 195–201.
35. Kiefer, F.; Arnold, K.; Kunzli, M.; Bordoli, L.; Schwede, T. *Nucleic Acids Res.* **2009**, *37*, D387–92.
36. Peitsch, M. C. *Biotechnology* **1995**, *13*, 658.
37. Eswar, N.; Webb, B.; Marti-Renom, M. A.; Madhusudhan, M. S.; Eramian, D.; Shen, M.; Pieper, U.; Sali, A. *Comparative Protein Structure Modeling with MODELLER*; John Wiley & Sons, Inc., 2006.
38. Huber, G. A.; McCammon, J. A. *Comput. Phys. Commun.* **2010**, *181*, 1896–1905.
39. Mereghetti, P.; Gabdoulline, R. R.; Wade, R. C. *Biophys. J.* **2010**, *99*, 3782–3791.
40. Frembgen-Kesner, T.; Elcock, A. H. *Biophys. J.* **2010**, *99*, L75–L77.
41. Gorecki, A.; Szypowski, M.; Dlugosz, M.; Trylska, J. *J. Comput. Chem.* **2009**, *30*, 2364–2373.
42. Kim, Y. C.; Hummer, G. *J. Mol. Biol.* **2008**, *375*, 1416–1433.
43. Carmichael, S. P.; Shell, M. S. *J. Phys. Chem. B* **2012**, *116*, 8383–8393.
44. Zheng, W. *J. Chem. Phys.* **2012**, *136*, 155103.
45. Trylska, J.; Tozzini, V.; Chang, C. A.; McCammon, J. A. *Biophys. J.* **2007**, *92*, 4179–4187.
46. Moussavi-Baygi, R.; Jamali, Y.; Karimi, R.; Mofrad, M. R. K. *PLoS Comput. Biol.* **2011**, *7*, 16.
47. Lu, L. Y.; Izvekov, S.; Das, A.; Andersen, H. C.; Voth, G. A. *J. Chem. Theor. Comput.* **2010**, *6*, 954–965.
48. Chu, J. W.; Izveko, S.; Voth, G. A. *Mol. Simul.* **2006**, *32*, 211–218.
49. Davtyan, A.; Schafer, N. P.; Zheng, W.; Clementi, C.; Wolynes, P. G.; Papoian, G. A. *J. Phys. Chem. B* **2012**, *116*, 8494–8503.
50. Clementi, C. *Curr. Opin. Struct. Biol.* **2008**, *18*, 10–15.
51. Samiotakis, A.; Homouz, D.; Cheung, M. S. *J. Chem. Phys.* **2010**, *132*, 175101.
52. Gopal, S. M.; Mukherjee, S.; Cheng, Y. M.; Feig, M. *Proteins Struct. Funct. Bioinform.* **2010**, *78*, 1266–1281.
53. Savelyev, A.; Papoian, G. A. *Biophys. J.* **2009**, *96*, 4044–4052.
54. Kamerlin, S. C. L.; Vicatos, S.; Dryga, A.; Warshel, A. In: Leone, S. R.; Cremer, P. S.; Groves, J. T.; Johnson, M. A., Eds.; Annual Review of Physical Chemistry, Vol. 62; Annual Reviews: Palo Alto, **2011**; pp 41–64.
55. Wang, Q.; Cheung, M. S. *Biophys. J.* **2012**, *102*, 2353–2361.
56. Marrink, S. J.; Risselada, H. J.; Yefimov, S.; Tieleman, D. P.; de Vries, A. H. *J. Phys. Chem. B* **2007**, *111*, 7812–7824.
57. Kang, M.; Roberts, C.; Cheng, Y.; Chang, C.-e. A. *J. Chem. Theor. Comput.* **2011**, *7*, 3438–3446.
58. Tozzini, V.; McCammon, J. A. *Chem. Phys. Lett.* **2005**, *413*, 123–128.
59. Wang, P.; Byeon, I. J. L.; Liao, H.; Beebe, K. D.; Yongkiettrakul, S.; Pei, D.; Tsai, M. D. *J. Mol. Biol.* **2000**, *302*, 927–940.
60. Liao, H.; Byeon, I. J. L.; Tsai, M. D. *J. Mol. Biol.* **1999**, *294*, 1041–1049.

61. Durocher, D.; Taylor, I. A.; Sarbassova, D.; Haire, L. F.; Westcott, S. L.; Jackson, S. P.; Smerdon, S. J.; Yaffe, M. B. *Mol. Cell* **2000**, *6*, 1169–1182.
62. Mahajan, A.; Yuan, C. H.; Lee, H.; Chen, E. S. W.; Wu, P. Y.; Tsai, M. D. *Sci. Signal.* **2009**, *2*, re12.
63. Pennell, S.; Westcott, S.; Ortiz-Lombardia, M.; Patel, D.; Li, J.; Nott, T. J.; Mohammed, D.; Buxton, R. S.; Yaffe, M. B.; Verma, C.; Smerdon, S. J. *Structure* **2010**, *18*, 1587–1595.
64. Leung, C. S.; Leung, S. S. F.; Tirado-Rives, J.; Jorgensen, W. L. *J. Med. Chem.* **2012**, *55*, 4489–4500.
65. Lee, S. J.; Schwartz, M. F.; Duong, J. K.; Stern, D. F. *Mol. Cell. Biol.* **2003**, *23*, 6300–6314.
66. Lee, H.; Yuan, C. H.; Hammet, A.; Mahajan, A.; Chen, E. S. W.; Wu, M. R.; Su, M. I.; Heierhorst, J.; Tsai, M. D. *Mol. Cell* **2008**, *30*, 767–778.
67. Hofmann, K.; Bucher, P. *Trends Biochem. Sci.* **1995**, *20*, 347–349.
68. Joshi, M.; Ebalunode, J. O.; Briggs, J. M. *Proteins Struct. Funct. Bioinform.* **2009**, *75*, 323–335.
69. Clapperton, J. A.; Manke, I. A.; Lowery, D. M.; Ho, T.; Haire, L. F.; Yaffe, M. B.; Smerdon, S. J. *Nat. Struct. Mol. Biol.* **2004**, *11*, 512–518.
70. Shiozaki, E. N.; Gu, L. C.; Yan, N.; Shi, Y. G. *Mol. Cell* **2004**, *14*, 405–412.
71. Varma, A. K.; Brown, R. S.; Birrane, G.; Ladias, J. A. A. *Biochemistry* **2005**, *44*, 10941–10946.
72. Shen, Y.; Tong, L. *Biochemistry* **2008**, *47*, 5767–5773.
73. Meng, W. Y.; Sawasdikosol, S.; Burakoff, S. J.; Eck, M. J. *Nature* **1999**, *398*, 84–90.
74. Tronrud, D. E.; Wen, J.; Gay, L.; Blankenship, R. E. *Photosynth. Res.* **2009**, *100*, 79–87.
75. Yuan, C. H.; Yongkiettrakul, S.; Byeon, I. J. L.; Zhou, S. Z.; Tsai, M. D. *J. Mol. Biol.* **2001**, *314*, 563–575.
76. Byeon, I. J. L.; Yongkiettrakul, S.; Tsai, M. D. *J. Mol. Biol.* **2001**, *314*, 577–588.
77. Lee, G. I.; Ding, Z. F.; Walker, J. C.; Van Doren, S. R. *Proc. Natl. Acad. Sci. U. S. A.* **2003**, *100*, 11261–11266.
78. Ali, A. A. E.; Jukes, R. M.; Pearl, L. H.; Oliver, A. W. *Nucleic Acids Res.* **2009**, *37*, 1701–1712.
79. Nott, T. J.; Kelly, G.; Stach, L.; Li, J. J.; Westcott, S.; Patel, D.; Hunt, D. M.; Howell, S.; Buxton, R. S.; O'Hare, H. M.; Smerdon, S. J. *Sci. Signal.* **2009**, *2*, ra12.
80. Huang, Y.-m. M.; Chang, C.-e. A. *BMC Biophys.* **2011**, *4*, 12.
81. Otte, L.; Wiedemann, U.; Schlegel, B.; Pires, J. R.; Beyermann, M.; Schmieder, P.; Krause, G.; Volkmer-Engert, R.; Schneider-Mergener, J.; Oschkinat, H. *Protein Sci.* **2003**, *12*, 491–500.
82. Lu, P. J.; Zhou, X. Z.; Liou, Y. C.; Noel, J. P.; Lu, K. P. *J. Biol. Chem.* **2002**, *277*, 2381–2384.
83. Verdecia, M. A.; Bowman, M. E.; Lu, K. P.; Hunter, T.; Noel, J. P. *Nat. Struct. Biol.* **2000**, *7*, 639–643.
84. Mittermaier, A. K.; Kay, L. E. *Trends Biochem. Sci.* **2009**, *34*, 601–611.
85. Boehr, D. D.; Dyson, H. J.; Wright, P. E. *Chem. Rev.* **2006**, *106*, 3055–3079.
86. Palmer, A. G.; Massi, F. *Chem. Rev.* **2006**, *106*, 1700–1719.
87. Morcos, F.; Chatterjee, S.; McClendon, C. L.; Brenner, P. R.; Lopez-Rendon, R.; Zintsmaster, J.; Ercsey-Ravasz, M.; Sweet, C. R.; Jacobson, M. P.; Peng, J. W.; Izaguirre, J. A. *PLoS Comput. Biol.* **2010**, *6*, e1001015.
88. Okazaki, K.-i.; Takada, S. *Proc. Natl. Acad. Sci. U. S. A.* **2008**, *105*, 11182–11187.
89. Koshland, D. E. *Proc. Natl. Acad. Sci. U. S. A.* **1958**, *44*, 98–104.
90. Fischer, E. *Ber. Dtsch. Chem. Ges.* **1894**, *27*, 2984–2993.

91. Lee, B. M.; Xu, J.; Clarkson, B. K.; Martinez-Yamout, M. A.; Dyson, H. J.; Case, D. A.; Gottesfeld, J. M.; Wright, P. E. *J. Mol. Biol.* **2006**, *357*, 275–291.
92. Kushwaha, P. S.; Mishra, P. C. *Int. J. Quantum Chem.* **2000**, *76*, 700–713.
93. Jorgensen, W. L. *Science* **1991**, *254*, 954–955.
94. Kar, G.; Keskin, O.; Gursoy, A.; Nussinov, R. *Curr. Opin. Pharmacol.* **2010**, *10*, 715–722.
95. Callebaut, I.; Mornon, J. P. *FEBS Lett.* **1997**, *400*, 25–30.
96. Huang, Y.-m. M.; Kang, M.; Chang, C.-e. A. *J. Phys. Chem. B* **2012**, *116*, 10247–10258.
97. Glover, J. N. M.; Williams, R. S.; Lee, M. S. *Trends Biochem. Sci.* **2004**, *29*, 579–585.
98. Williams, R. S.; Green, R.; Glover, J. N. M. *Nat. Struct. Biol.* **2001**, *8*, 838–842.
99. Watts, F. Z.; Brissett, N. C. *DNA Repair* **2010**, *9*, 103–108.
100. Gorfe, A. A.; Chang, C. E. A.; Ivanov, I.; McCammon, J. A. *Biophys. J.* **2008**, *94*, 1144–1154.
101. Held, M.; Noe, F. *Eur. J. Cell Biol.* **2012**, *91*, 357–364.
102. Elber, R. *Curr. Opin. Struct. Biol.* **2010**, *20*, 162–167.
103. Naramura, M.; Nadeau, S.; Mohapatra, B.; Ahmad, G.; Mukhopadhyay, C.; Sattler, M.; Raja, S. M.; Natarajan, A.; Band, V.; Band, H. *Oncotarget* **2011**, *2*, 245–250.
104. Ng, C.; Jackson, R. A.; Buschdorf, J. P.; Sun, Q. X.; Guy, G. R.; Sivaraman, J. *EMBO J.* **2008**, *27*, 804–816.
105. Kumar, E. A.; Yuan, Z.; Palermo, N. Y.; Dong, L.; Ahmad, G.; Lokesh, G. L.; Kolar, C.; Kizhake, S.; Borgstahl, G. E. O.; Band, H.; Natarajan, A. *J. Med. Chem.* **2012**, *55*, 3583–3587.